Published in final edited form as:
Neuromuscul Disord. 2011 January ; 21(1): 68–73. doi:10.1016/j.nmd.2010.09.007.

Magnetic Resonance Imaging Assessment of Cardiac Dysfunction in δ-Sarcoglycan Null Mice

Janaka P. Wansapura, PhD[1], **Douglas P. Millay, PhD**[2], **R. Scott Dunn, RT**[1], **Jeffery D. Molkentin, PhD**[2], and **D. Woodrow Benson, MD, PhD**[2,3]

[1]Department of Radiology / Imaging Research Center, Cincinnati Children's Hospital Medical Center, Cincinnati, Ohio

[2]Division of Molecular Cardiovascular Biology, Cincinnati Children's Hospital Medical Center, Cincinnati, Ohio

[3]Division of Cardiology, Cincinnati Children's Hospital Medical Center, Cincinnati, Ohio

Abstract

Delta-sarcoglycan null, *Scgd*$^{-/-}$, mice develop cardiac and skeletal muscle histopathological alterations similar to those in humans with limb girdle muscular dystrophy. The objective of this study was to assess the feasibility of using MRI to investigate cardiac dysfunction in *Scgd*$^{-/-}$ mice. Cardiac MRI of 8 month old *Scgd*$^{-/-}$ and wild type, WT mice was performed. Compared to WT, *Scgd*$^{-/-}$ mice had significantly lower LV ejection fraction (44±5% vs. 66±4% p=0.014), lower RV ejection fraction (25±2% vs. 51±3%, p<0.001) lower myocardial circumferential strain, (15.0±0.3% vs. 16.9±0.3%, p=0.007) and RV dilatation (54±3μL vs. 40±3μL, p=0.007). The regional circumferential strain also demonstrated significant temporal dyssynchrony between opposing regions of the *Scgd*$^{-/-}$ LV. Our results demonstrate severe cardiac dysfunction in *Scgd*$^{-/-}$ mice at 8 months. The study identifies a set of non invasive markers that could be used to study efficacy of novel therapeutic agents in muscular dystrophic mice.

Keywords

limb-girdle muscular dystrophy; sarcoglycan null; cardiac function; dyssynchrony

INTRODUCTION

The most commonly used laboratory model of muscular dystrophy is the C57Bl/10ScSn mdx (mdx) mouse. Whilst the mdx is a genetic homologue of Duchenne muscular dystrophy (DMD), cardiac and skeletal muscle pathology is comparatively moderate resulting in an almost normal lifespan. The δ-sarcoglycan null (*Scgd*$^{-/-}$) mouse on the other hand is a model of severe dystrophy in both cardiac and skeletal muscle [1]. Sarcoglycans are transmembrane proteins that compose the dystrophin-glycoprotein complex (DGC). The

Corresponding Author: Janaka Wansapura, PhD Cincinnati Children's Hospital Medical Center Department of Radiology / Imaging Research Center 3333 Burnet Ave. MLC 5033 Cincinnati, OH USA. Phone: (513) 636 9384 Fax: (513) 636 3754 janaka.wansapura@cchmc.org.

DGC is a large protein complex that affixes the basal lamina outside the cell to the contractile protein within the cell. A number of diverse genetic mutations within the DGC results in muscular dystrophy. Mutations in α, β, γ and δ-sarcoglycan in particular cause autosomal recessive limb-girdle muscular dystrophy (LGMD)[2] and have been associated with cardiac dysfunction [3–4]. *Scgd*$^{-/-}$ mice show skeletal muscle histopathology similar to human LGMD and develop focal areas of myocardial necrosis[1]. The exact role of dystrophin and DGC is unclear but the absence of these proteins is thought to perturb the linkage between the extracellular matrix and the muscle cell rendering the sarcolemma unstable against physical force[2,5]. .

In this study we used Magnetic Resonance Imaging (MRI) to characterize the cardiac phenotype of the *Scgd*$^{-/-}$ mouse. Previous studies have demonstrated the utility of MRI in the assessment of cardiac morphology and function in myopathic mouse models [6–7]. However these studies have limited their functional assessment to the evaluation of ejection fraction and cardiac output. These global indices may not be as sensitive as the measures of local myocardial strain to the effects of local forces acting on the left ventricle. Several studies have demonstrated that dystrophin-defected skeletal muscle cells are abnormally vulnerable to stretch[8–9] Since deficiency in sarcoglycan protein increases susceptibility to contraction-induced sarcolemmal rupture, myocardial strain could be impaired in the *Scgd*$^{-/-}$ mouse in regions where local mechanical stress is high. Thus, we used high resolution MR tagging to measure circumferential strain and spatiotemporal dyssynchrony in addition to global ventricular function in the *Scgd*$^{-/-}$ heart. MR tagging is an imaging technique used to quantify tissue deformation [10]. Previously we have demonstrated the utility of this technique in mouse models of cardiac disease [11–12]. Our motivation for investigating circumferential strain in this study was based on a previous study of DMD boys in which we found that peak left ventricular composite myocardial circumferential strain is reduced early in the course of the disease despite normal ejection fraction and that circumferential strain continue to decline with advancing age [13].

MATERIALS AND METHODS

Animals

MR imaging was performed on 8 month old C57BL10 (*WT*) and age-matched, *Scgd*$^{-/-}$ mice bred at our institute. We selected animals at 8 months of age because previous studies indicated that obvious manifestations of disease are present by this age. The study was conducted under a protocol approved by the Institutional Animal Care and Use Committee.

Cardiac Function

Delayed enhancement, tagging and functional imaging were performed on eight months old wild type (*WT*) (n=5), and *Scgd*$^{-/-}$ (n=5) mice. Image acquisition was prospectively ECG gated using pediatric ECG probes attached to the paws. A pneumatic pillow was used for respiratory gating.

A bolus of Gd-DTPA (0.3–0.6 mmol/kg) was given intraperitonealy while the mouse was placed in the scanner bore. Delayed enhancement MR was performed using a T1 weighted (achieved by increasing the flip angle to 30°–40°) cine sequence. The hyper enhancement retained in the affected mouse heart for 40–50 minutes reaching a peak at around 30 minutes. This long enhancement period allowed a multi slice T1 weighted cine series to be acquired covering the entire left ventricle. Cine imaging was performed in the short axis using a segmented FLASH sequence. Slice thickness=1.0 mm, matrix size=256×256, in-plane resolution=117×117 μm^2. TE/TR=3/5.2ms, flip angle=20°, segments=1. Approximately 15–20 cine frames were acquired during the cardiac cycle with a temporal

resolution of TR ms. Tagged images were acquired in the mid ventricle. The spatial modulation of magnetization was achieved by a pulse train consist of 5 rectangular 0.1ms RF pulses with flips 10°, 30°, 50°, 30° and 10°. Cine images were acquired using an ECG gated, segmented FLASH sequence. Imaging parameters are as follows: TE/TR=1.85/7.1 ms, Tag separation=0.8 mm, FOV=34×34 mm^2, slice thickness=1 mm, Matrix=256×128. Horizontal and vertical tag lines were acquired separately with read direction perpendicular to the tag orientation. Images were reconstructed to a 256×256 matrix and then converted to DICOM format.

Image processing was done using custom built software called MICE (CCHMC, Cincinnati, OH) programmed in the IDL (IDL 6.2, ITT Visual Information Solutions, Boulder, CO) environment. Myocardial strain analysis was performed using HARP (Diagnosoft Plus, Diagnosoft Inc., CA, USA). Ventricular end diastolic volumes, LV and RV ejection fractions (LVEF, RVEF) mean myocardial Eularian circumferential strain (Ecc), cross correlation delay time [14–15] (XCD) were calculated and compared between the two groups. Results are expressed as mean ± SEM. Statistical differences were assessed with the unpaired 2-tailed Student's t test for two experimental groups, using SigmaStat (SPSS) software. A nonparametric test was applied when the data were not normally distributed. A 2-tailed P value of less than 0.05 was considered statistically significant.

RESULTS

FLASH cine images clearly demonstrated the abnormal structure and function of *Scgd*$^{-/-}$ hearts (Figure 1). Results are summarized in Table 1. The LV weight of *Scgd*$^{-/-}$ mice (0.101±0.003g) was significantly (p=0.003) greater than that of *WT* (0.080±0.005g), but LV end diastolic volume of *Scgd*$^{-/-}$ mice (86±12μL) was not significantly (p=0.31) different than that of *WT* (73±2μL). However, RV end diastolic volume of *Scgd*$^{-/-}$ mice, (54±3μL) was significantly (p=0.007) larger than that of *WT* (40±3μL). The *Scgd*$^{-/-}$ mouse had significantly low LV (p=0.014) and RV (p<0.001) ejection fractions compared to *WT* mice (Figure 2). LVEF=66±4% *WT* and LVEF=44±5% Scgd$^{-/-}$, RVEF=51±3% *WT* and RVEF=25±2% *Scgd*$^{-/-}$. The resting heart rates were similar between the two groups.

Myocardial strain analysis showed regional and global functional impairment in *Scgd*$^{-/-}$ hearts. The maximum global Eulerian circumferential strain of the LV at mid ventricular level, |Ecc| was significantly (p=0.007) lower in the *Scgd*$^{-/-}$ (=15.0±0.3%) than in the *WT* (=16.9± 0.3%) (Figure 3). The regional Ecc also demonstrated significant temporal dyssynchrony between opposing regions of the *Scgd*$^{-/-}$ LV as evident from the maximum cross correlation delay, XCD. The Ecc derived XCD was significantly (p<0.001) higher for the *Scgd*$^{-/-}$ (=55±3ms) than it was for the *WT* (=8±5ms).

Only one *Scgd*$^{-/-}$ mouse showed clear evidence of delayed enhancement (Figure 4). No delayed enhancement was seen in the *WT*.

DISCUSSION

Previous studies by Coral-Vazquez et al [1] have shown that *Scgd*$^{-/-}$ mouse develop skeletal muscle dystrophy and cardiomyopathy; histopathology demonstrated focal areas of necrosis in cardiac and skeletal muscle. Premature death begins to occur around 6 months of age. To our knowledge, this is the first in vivo imaging study examining the cardiac morphology and function of the *Scgd*$^{-/-}$ mouse. Our results confirm the previous assertion that the disruption of δ-sarcoglycan gene causes severe adverse response in cardiac function and morphology in the *Scgd*$^{-/-}$ mouse.

The utility of cine MRI in the assessment of cardiac morphology and function in myopathic mouse models has been previously described [6–7]. Typically in the *mdx* mouse, a commonly used model of human muscular dystrophy, the systolic function is found to be normal even at 8 months of age [7]. In contrast, we found that the 8 month old *Scgd*$^{-/-}$ mouse had reduced LV ejection fraction when compared to wild type. We also found that *Scgd*$^{-/-}$ had significant RV dilatation and reduced RV ejection, an observation that has not been previously reported in *Scgd*$^{-/-}$ mice. Coral-Vazquez et al [1] found severe necrosis in the young *Scgd*$^{-/-}$ diaphragm. The diaphragm muscle weakness could lead to pulmonary dysfunction and RV dilatation. Interestingly pulmonary dysfunction is common in the advanced stages of Duchenne muscular dystrophy and limb-girdle muscular dystrophy patients [16–18].

In addition to cine MRI we performed delayed enhanced MR (MDE) imaging and myocardial tagging. Only one out of five *Scgd*$^{-/-}$ mice showed positive MDE. A mild increase in signal intensity was seen in the anterior lateral and septal wall at basal level (Figure 4). The diffused pattern of signal distribution was markedly different to the well defined, high contrasted hyper enhancement typically seen in an ischemia reperfusion model. The diffused pattern of myocardial hyper enhancement is typical in older patients with muscular dystrophy and is well described in literature [19–24].

Due to long T1 relaxation times at 7 Tesla, myocardial tags persist throughout the cardiac cycle allowing accurate measurement of temporal evolution of myocardial strain in mice. Our results showed significant difference in Ecc between the *Scgd*$^{-/-}$ and WT mice. Progressive myocardial strain impairment has been observed in Duchenne muscular dystrophic patients [25]. In our experience, myocardial strain impairment precedes global dysfunction and could serve as an early sign of cardiomyopathy in these patients. We also measured a significantly high cross correlation delay, XCD in the *Scgd*$^{-/-}$ mice (55±3ms vs. 8±5ms). Studies with Doppler tissue imaging and phase contrast MRI has shown that XCD is superior to existing parameters at discriminating patients with left ventricular dyssynchrony from those with normal function [14–15]. The left ventricular dyssynchrony in *Scgd*$^{-/-}$ mice correlates well with Coral-Vazquez et al [1]'s observations in ECG characteristics of these mice. They found that ventricular excitation (QRS amplitude and duration) was markedly perturbed in Scgd$^{-/-}$ compared to WT consistent with the idea that fibrotic lesions in *Scgd*$^{-/-}$ underlie abnormal activation.

In summery, 8 months old *Scgd*$^{-/-}$ mice demonstrated both RV and LV dysfunction, RV dilatation, myocardial strain impairment and LV dyssynchrony. This study shows that myocardial strain quantified by MR tagging is a sensitive measure of regional impairment in these mice. Impaired myocardial strain points to damaged tissue structure. Since contraction induced myocardial injury plays a significant role in the pathobiology of this disease, it is important to be able to quantify this phenomenon non-invasively. Results of this study indicate that circumferential strain could be used as a surrogate marker of the disease severity. This could be particularly important in the pre-clinical assessment of novel therapeutic agents. On going research in this area at our center include longitudinal MRI study of *Scgd*$^{-/-}$ mice treated with a TGFβ blocking agent, Losartan. It is hoped that results of this study will further reveal the underlying pathobiology of the impaired function in these mice.

Studies have repeatedly shown that cardiac assessment by standard echocardiographic imaging is inadequate for detecting the presence of heart disease in the first decade of life[25–26]. Indeed, one of the limitations to assessing therapeutic effect in the early stages of cardiomyopathy has been the lack of sensitive diagnostic tools to identify cardiac dysfunction in the young patient. Myocardial strain can be assessed in routine clinical MRI

exams. Detection of strain abnormalities might provide a useful surrogate index to assess therapeutic efficacy.

REFERENCES

1. Coral-Vazquez R, Cohn RD, Moore SA, et al. Disruption of the sarcoglycan-sarcospan complex in vascular smooth muscle: a novel mechanism for cardiomyopathy and muscular dystrophy. Cell 1999;98:465–74. [PubMed: 10481911]
2. Lim LE, Campbell KP. The sarcoglycan complex in limb-girdle muscular dystrophy. Curr Opin Neurol 1998;11:443–52. [PubMed: 9847993]
3. Fanin M, Melacini P, Boito C, Pegoraro E, Angelini C. LGMD2E patients risk developing dilated cardiomyopathy. Neuromuscul Disord 2003;13:303–9. [PubMed: 12868499]
4. Melacini P, Fanin M, Duggan DJ, et al. Heart involvement in muscular dystrophies due to sarcoglycan gene mutations. Muscle Nerve 1999;22:473–9. [PubMed: 10204782]
5. Durbeej M, Campbell KP. Muscular dystrophies involving the dystrophin-glycoprotein complex: an overview of current mouse models. Curr Opin Genet Dev 2002;12:349–61. [PubMed: 12076680]
6. Wilding JR, Schneider JE, Sang AE, Davies KE, Neubauer S, Clarke K. Dystrophin- and MLP-deficient mouse hearts: marked differences in morphology and function, but similar accumulation of cytoskeletal proteins. FASEB J 2005;19:79–81. [PubMed: 15494447]
7. Zhang W, ten Hove M, Schneider JE, et al. Abnormal cardiac morphology, function and energy metabolism in the dystrophic mdx mouse: an MRI and MRS study. J Mol Cell Cardiol 2008;45:754–60. [PubMed: 18929569]
8. Moens P, Baatsen PH, Marechal G. Increased susceptibility of EDL muscles from mdx mice to damage induced by contractions with stretch. J Muscle Res Cell Motil 1993;14:446–51. [PubMed: 7693747]
9. Petrof BJ, Shrager JB, Stedman HH, Kelly AM, Sweeney HL. Dystrophin protects the sarcolemma from stresses developed during muscle contraction. Proc Natl Acad Sci U S A 1993;90:3710–4. [PubMed: 8475120]
10. Axel L, Dougherty L. MR imaging of motion with spatial modulation of magnetization. Radiology 1989;171:841–5. [PubMed: 2717762]
11. Diwan A, Wansapura J, Syed FM, Matkovich SJ, Lorenz JN, Dorn GW 2nd. Nix-mediated apoptosis links myocardial fibrosis, cardiac remodeling, and hypertrophy decompensation. Circulation 2008;117:396–404. [PubMed: 18178777]
12. Diwan A, Krenz M, Syed FM, et al. Inhibition of ischemic cardiomyocyte apoptosis through targeted ablation of Bnip3 restrains postinfarction remodeling in mice. J Clin Invest 2007;117:2825–33. [PubMed: 17909626]
13. Hor KN, Wansapura J, Markham LW, et al. Circumferential strain analysis identifies strata of cardiomyopathy in Duchenne muscular dystrophy: a cardiac magnetic resonance tagging study. J Am Coll Cardiol 2009;53:1204–10. [PubMed: 19341862]
14. Fornwalt BK, Arita T, Bhasin M, et al. Cross-correlation quantification of dyssynchrony: a new method for quantifying the synchrony of contraction and relaxation in the heart. J Am Soc Echocardiogr 2007;20:1330–7. e1. [PubMed: 17643956]
15. Delfino JG, Fornwalt BK, Eisner RL, Leon AR, Oshinski JN. Cross-correlation delay to quantify myocardial dyssynchrony from phase contrast magnetic resonance (PCMR) velocity data. J Magn Reson Imaging 2008;28:1086–91. [PubMed: 18972349]
16. Hahn A, Bach JR, Delaubier A, Renardel-Irani A, Guillou C, Rideau Y. Clinical implications of maximal respiratory pressure determinations for individuals with Duchenne muscular dystrophy. Arch Phys Med Rehabil 1997;78:1–6. [PubMed: 9014949]
17. Melacini P, Vianello A, Villanova C, et al. Cardiac and respiratory involvement in advanced stage Duchenne muscular dystrophy. Neuromuscul Disord 1996;6:367–76. [PubMed: 8938701]
18. Poppe M, Cree L, Bourke J, et al. The phenotype of limb-girdle muscular dystrophy type 2I. Neurology 2003;60:1246–51. [PubMed: 12707425]
19. Petrie CJ, Mark PB, Dargie HJ. Cardiomyopathy in Becker muscular dystrophy--does regional fibrosis mimic infarction? J Cardiovasc Magn Reson 2005;7:823–5. [PubMed: 16353443]

20. Guillaume MD, Phoon CK, Chun AJ, Srichai MB. Delayed enhancement cardiac magnetic resonance imaging in a patient with Duchenne muscular dystrophy. Tex Heart Inst J 2008;35:367–8. [PubMed: 18941638]

21. Varghese A, Pennell DJ. Late gadolinium enhanced cardiovascular magnetic resonance in Becker muscular dystrophy. Heart 2004;90:e59. [PubMed: 15310728]

22. Puchalski MD, Williams RV, Askovich B, et al. Late gadolinium enhancement: precursor to cardiomyopathy in Duchenne muscular dystrophy? Int J Cardiovasc Imaging 2009;25:57–63. [PubMed: 18686011]

23. Suselbeck T, Haghi D, Neff W, Borggrefe M, Papavassiliu T. Midwall myocardial fibrosis in Becker-Kiener muscular dystrophy. Z Kardiol 2005;94:465–8. [PubMed: 15997348]

24. Silva MC, Meira ZM, Gurgel Giannetti J, et al. Myocardial delayed enhancement by magnetic resonance imaging in patients with muscular dystrophy. J Am Coll Cardiol 2007;49:1874–9. [PubMed: 17481447]

25. Ashford MW Jr. Liu W, Lin SJ, et al. Occult cardiac contractile dysfunction in dystrophin-deficient children revealed by cardiac magnetic resonance strain imaging. Circulation 2005;112:2462–7. [PubMed: 16216964]

26. Schreiber A, Smith WL, Ionasescu V, et al. Magnetic resonance imaging of children with Duchenne muscular dystrophy. Pediatr Radiol 1987;17:495–7. [PubMed: 3684364]

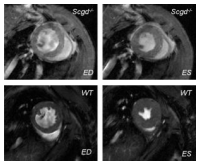

Figure 1.
FLASH images in the short axis view at end diastole (ED) and end systole (ES) clearly show enlarged ventricular chambers of the Scgd$^{-/-}$ mouse. LV and RV ejection fractions were significantly low in the Scgd$^{-/-}$ mouse.

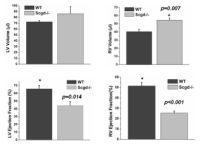

Figure 2.

Compared to WT, Scgd$^{-/-}$ mouse showed higher end diastolic LV (by 19%) and RV (by 35%, p=0.007) volumes. Compared to WT, both LV and RV ejection fractions (LV by 33%, p=0.014 and RV by 51%, p<0.001) were significantly low in the Scgd$^{-/-}$ mouse.

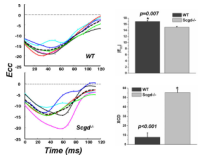

Figure 3.

The time evolution of mid ventricular circumferential strain (Ecc) in 6 different LV regions (colored lines) show significant dyssynchrony in the Scgd$^{-/-}$ hearts and is quantified by XCD ($p<0.001$). The mean Ecc (broken line) is significantly ($p=0.007$) low in Scgd$^{-/-}$ compared to WT.

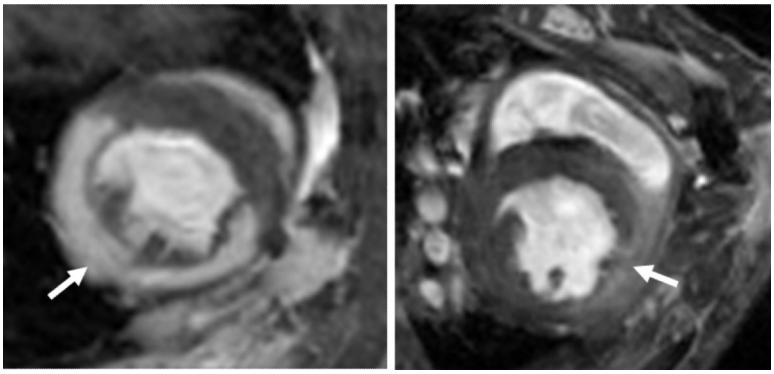

Figure 4.

Delayed enhanced, T1wt short axis images of an ischemia reperfusion (IR) mouse model (left) and the Scgd$^{-/-}$ (right) show marked difference in the enhancement pattern. In the IR mouse, the hyper-enhancement is greater and the region is well defined while in the Scgd$^{-/-}$ mouse, the enhancement is less and diffused.

Table 1

Summary of MRI derived indices.

	Scgd$^{-/-}$	WT	P value
LV weight (gm)	0.101±0.003	0.080±0.005	0.003
LVEDV (μL)	86±12	73±2	NS
RVEDV (μL)	54±3	40±3	0.007
LVEF (%)	44±5	66±4	0.014
RVEF (%)	25±2	51±3	<0.001
Ecc (%)	15.0±0.3	16.9±0.3	0.007
XCD (ms)	55±3	8±5	<0.001

LV weight: Left ventricular weight, LVED: Left ventricular end diastolic volume, RVEDV: Right ventricular end diastolic volume, LVEF: Left ventricular ejection fraction, RVEF: Right ventricular ejection fraction, Ecc: Circumferential strain, XCD: Cross correlation delay.